Life Sciences 239 (2019) 117015

Contents lists available at ScienceDirect

Life Sciences

journal homepage: www.elsevier.com/locate/lifescie

Aldehyde dehydrogenase-2 acts as a potential genetic target for renal fibrosis

Simin Tang[b,c,1], Teng Huang[b,1], Huan Jing[b,d], Zhenxing Huang[b], Hongtao Chen[e], Youling Fan[f], Jiying Zhong[b], Jun Zhou[a,*]

[a] Department of Anesthesiology, The Third Affiliated Hospital of Southern Medical University, Guangzhou, Guangdong Province, 510000, China
[b] Department of Anesthesiology, The First People's Hospital of Foshan, Foshan, Guangdong Province, 528000, China
[c] Sun Yet-Sen Memorial Hospital of Sun Yet-Sen University, Guangzhou, Guangdong Province, 510000, China
[d] ZunYi Medical University, ZunYi, Guizhou Province, 563100, China
[e] Department of Anesthesiology, Guangzhou Eighth People's Hospital, Guangzhou Medical University, Guangzhou, Guangdong Province, 510060, China
[f] Department of Anesthesiology, Panyu Central Hospital, Guangzhou, Guangdong Province, 511400, China

ARTICLE INFO

Keywords:
Unilateral ureteral obstruction
Cisplatin
Ischemia-reperfusion injury
Renal fibrosis
Bioinformatics
Aldh2
Glycolysis pathway

ABSTRACT

Obstructive renal injury and drug-induced nephrotoxicity are the two most common causes of renal fibrosis diseases. However, whether these two different pathogeny induced same pathological outcomes contain common genetic targets or signaling pathway, the current research has not paid great attention. GSE121190 and GSE35257 were downloaded from the Gene Expression Omnibus (GEO) database. While GSE121190 represents a differential expression profile in kidney of mice with unilateral ureteral obstruction (UUO) model, GSE35257 represents cisplatin nephrotoxicity model. By using GEO2R, 965 differential expression genes (DEGs) in GSE121190 and 930 DEGs in GSE35257 were identified. 43 co-DEGs were shared and were extracted for protein-protein interaction (PPI) analysis. Subsequently, three shared pathways including glycolysis/gluconeogenesis, fatty acid degradation and pathways in cancer were involved in two models with Kyoto Encyclopedia of Genes and Genomes (KEGG) analysis. We reconfirmed that these three pathways have relatively high scores by using Gene Set Enrichment Analysis (GSEA) software. Additionally, further bioinformatic analysis showed that Aldehyde dehydrogenase-2 (Aldh2) involved in the progression of renal fibrosis by mediating glycolysis pathway. Then real-time PCR and western blotting were performed to validate the expression of Aldh2 in kidney tissue after three different etiologies that caused renal fibrosis. Basically consistent with our bioinformatics results, our experiment showed that the expression of Aldh2 is the most significantly decreased in the UUO model, followed by ischemia-reperfusion injury (IRI) model and finally the cisplatin-induced model. Thus, Aldh2 can act as a common potential genetic target for different renal fibrosis diseases.

1. Introduction

Renal fibrosis is the common terminal pathological changes of various kidney diseases [1]. As we know, chemical toxicity of drugs and obstructive mechanical damage cause genetic alterations of kidney, supporting molecular and cellular mechanisms in renal fibrosis pathogenesis [2]. Seeking the similarities and differences of targets and signaling pathway in the same ending caused by different etiologies is conducive to have a deeper understanding of molecular mechanisms of renal fibrosis. Unilateral ureteral obstruction (UUO) and the cisplatin-induced kidney injury are two classic animal models that can respectively represent obstructive nephropathy and pharmacotoxic nephropathy [3–5]. Two animal models of renal fibrosis have good reproducibility and are widely used in basic research of renal fibrosis currently.

Recently, with the rapid development of microarray and high-throughput sequencing technologies, the mechanisms of renal fibrosis at genomic levels were increasingly explored [6–8]. In the era of big data, it also provides us with a great convenience in analyzing gene functions with the increasingly sophisticated analysis techniques. In the present study, gene expression profiles of GSE121190 and GSE35257 were downloaded from the Gene Expression Omnibus (GEO) database. Three kidney samples of mice with UUO model and three kidney samples of mice with sham control were extracted from GSE121190,

* Corresponding author.
E-mail address: zhoujun7843@126.com (J. Zhou).
[1] Contributed equally.

https://doi.org/10.1016/j.lfs.2019.117015
Received 7 June 2019; Received in revised form 20 September 2019; Accepted 23 October 2019
Available online 31 October 2019

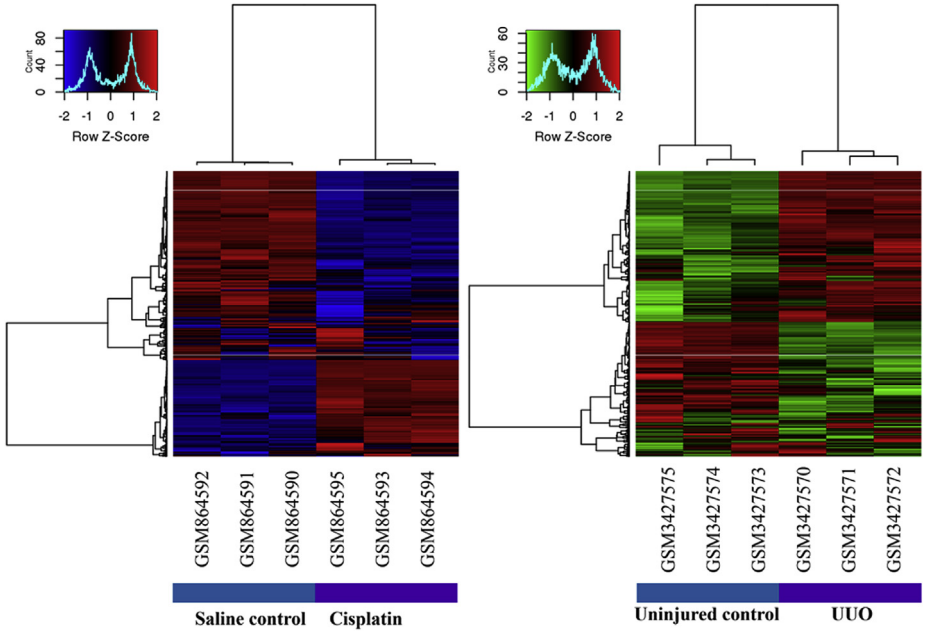

Fig. 1. Heatmap shows the distribution of gene expression data of each group extracted from GSE35257 and GSE121190. The difference distribution of the expression levels of each gene in different groups can be seen from the figure. Cluster analysis was performed on the basis of heatmap for groups and genes.

while three kidney samples of mice with cisplatin treatment and three normal kidney samples of mice were extracted from GSE35257. Both were selected to identify differential expression genes (DEGs) by using online tool GEO2R. Subsequently, Gene Ontology (GO) functions and Kyoto Encyclopedia of Genes and Genomes (KEGG) pathways of DEGs were analyzed and visualized in R software. The present study found that glycolysis/gluconeogenesis may be the key common pathway between obstructive renal injury and drug toxicity-induced renal fibrosis and only one shared gene Aldehyde dehydrogenase-2 (Aldh2) was found to involve in biological function of glycolysis/gluconeogenesis. In order to verify the commonality of Aldh2 in various renal fibrosis diseases, in addition to the above two models, we also added an ischemia-reperfusion injury (IRI) model to enhance the rigor of the experiment and the reliability of the results. Here, we then performed real-time PCR and western blotting to verify the gene expression of Aldh2 in three renal fibrosis models. In line with our bioinformatic results, our experiments showed that the expression of Aldh2 did have a significant downward trend after these three different causes. Specifically, we found that the expression of Aldh2 was most significantly decreased in the UUO model, followed by the IRI model and finally the cisplatin-induced model. Thus, our analysis indicated that Aldh2 act as a common potential genetic target for different renal fibrosis.

2. Materials and methods

2.1. Microarray data

GSE121190 and GSE35257 were downloaded from the GEO database (https://www.ncbi.nlm.nih.gov/geo/). While GSE121190 was based on the GPL11180 platform ([HT_MG-430_PM] Affymetrix HT MG-430 p.m. Array Plate), GSE35257 was based on the GPL6887 platform (Illumina MouseWG-6 v2.0 expression beadchip). In total, three UUO samples (GSM3427570, GSM3427571, GSM3427572) and three normal samples (GSM3427573, GSM3427574, GSM3427575) from GSE121190 and three cisplatin-induced samples (GSM864593, GSM864594, GSM864595) and three normal samples (GSM864590, GSM864591, GSM864592) from GSE35257 were selected. Subsequently, data quality was assessed from these two datasets by using R software.

2.2. Identification of DEGs

The online tool GEO2R (http://www.ncbi.nlm.nih.gov/geo/geo2r) was applied to screen DEGs. GEO2R is an intelligent web device that empowers clients to compare at least two datasets in a GEO series so as to distinguish DEGs [9]. The adjusted P-values (adj. P) and Benjamini and Hochberg false discovery rate were executed to give a harmony between disclosure of measurably huge qualities and impediments of false-positives. Probe sets without relating quality images or qualities with more than one probe set were evacuated or averaged, separately. Here, DEGs were screened and chosen by the cut-off point of adj.P $<$ 0.01 and $|\log FC| > 1$. Volcano and the heatmap were painted to picture these DEGs by using R ggplot2, and heatmap package.

2.3. Functional enrichment analyses

In order to find the substantial similar mechanisms between the two kinds of kidney injury pathogenesis, the DEGs from two datasets were then uploaded to the Database for Annotation, Visualization, and Integrated Discovery (DAVID) version 6.8 Beta (https://david-d.ncifcrf.gov/) for further analysis, respectively [10]. Gene ontology (GO) and Kyoto Encyclopedia of Gene and Genome (KEGG) pathways of DEGs were analyzed by using David and were pictured in R ggplot2 package. P-value $<$ 0.01 was considered statistically significant.

2.4. GSEA analysis

Subsequently, Gene Set Enrichment Analysis (GSEA) approach was applied to reconfirm KEGG pathway enrichment by analyzing the differential-expression data in GSEA software version 3.0 [11,12], which uses predefined gene sets from the Molecular Signatures Database (MSigDB v6.2). Then the results of three related KEGG pathways (glycolysis/gluconeogenesis; fatty acid degradation; pathways in cancer) were extracted and for further analysis.

2.5. PPI network construction

Additionally, Search Tool for the Retrieval of Interacting Genes (STRING; http://STRING-db.org) (version 11.0) online database [13]

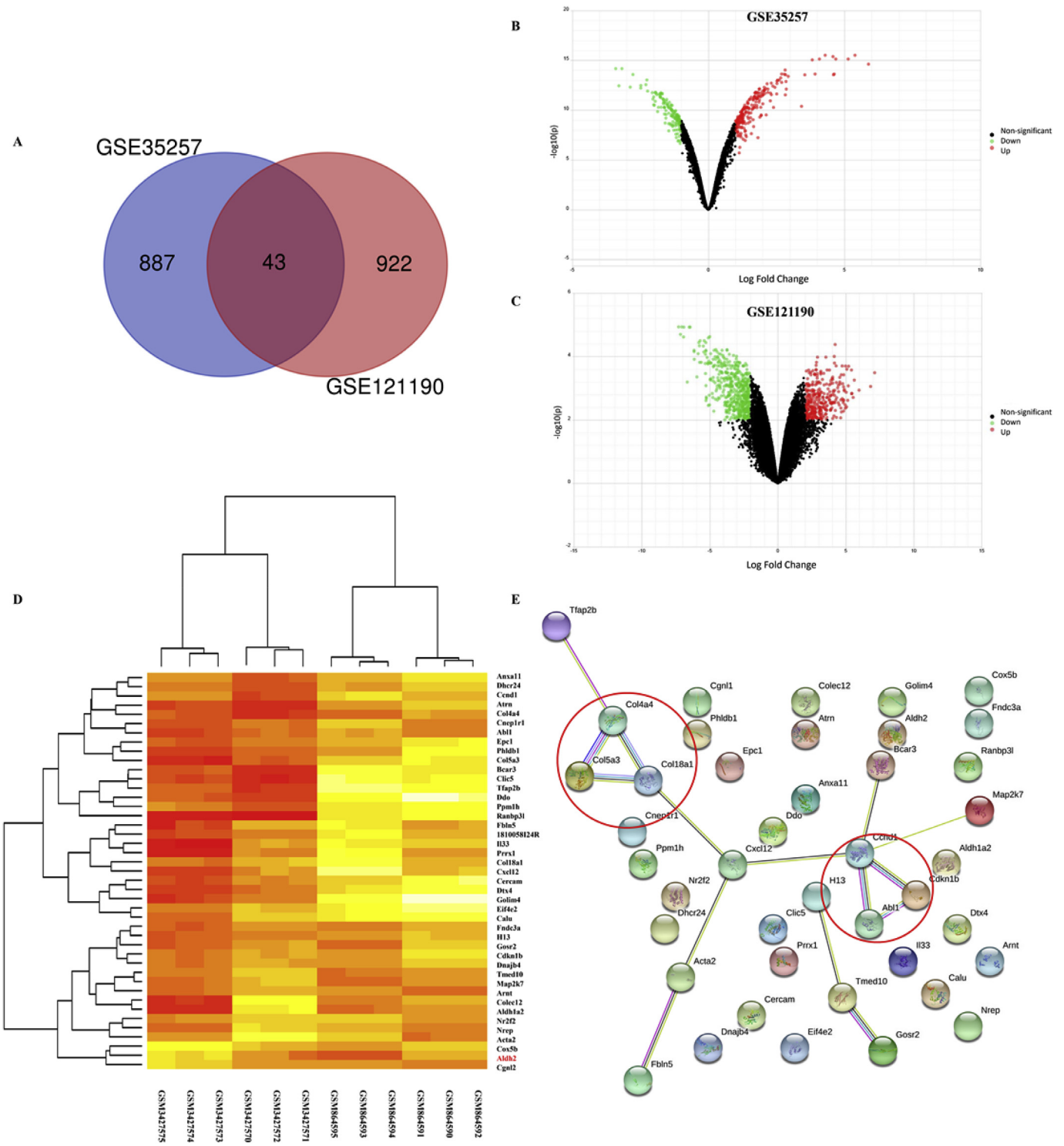

Fig. 2. Screening of DEGs and PPI network of 43 co-genes. A) Venn diagram showing 43 co-genes of the UUO DEGs and cisplatin-induced kidney injury DEGs. B) Volcano plot showing the UUO DEGs and cisplatin-induced kidney injury DEGs, respectively. C) Heatmap showing the expression change of 43 co-DEGs. D) PPI network of 45 co-DEGs showing the potential gene interaction by STRING database. The genes in Red circle may be hub genes. (For interpretation of the references to colour in this figure legend, the reader is referred to the Web version of this article.)

was applied to construct the protein–protein interaction (PPI) network of 45 co-DEGs to visualize the potential gene interaction network. It was also applied to lay bare the related genes involving in glycolysis/gluconeogenesis pathway by using its multiple proteins online tool, which can clearly reveal the shared gene involved in glycolysis/gluconeogenesis pathway in two animal models and their potential interactions.

2.6. Ingenuity pathway analysis

Ingenuity Pathway Analysis (IPA, https://www.qiagenbioinformatics.com/products/ingenuity-pathway-analysis/) is a system that exposes causal relationships of target genes associated with experimental data by using Overlay tool. In this study, we first built a comprehensive network of Aldh2 through IPA search function. Then we

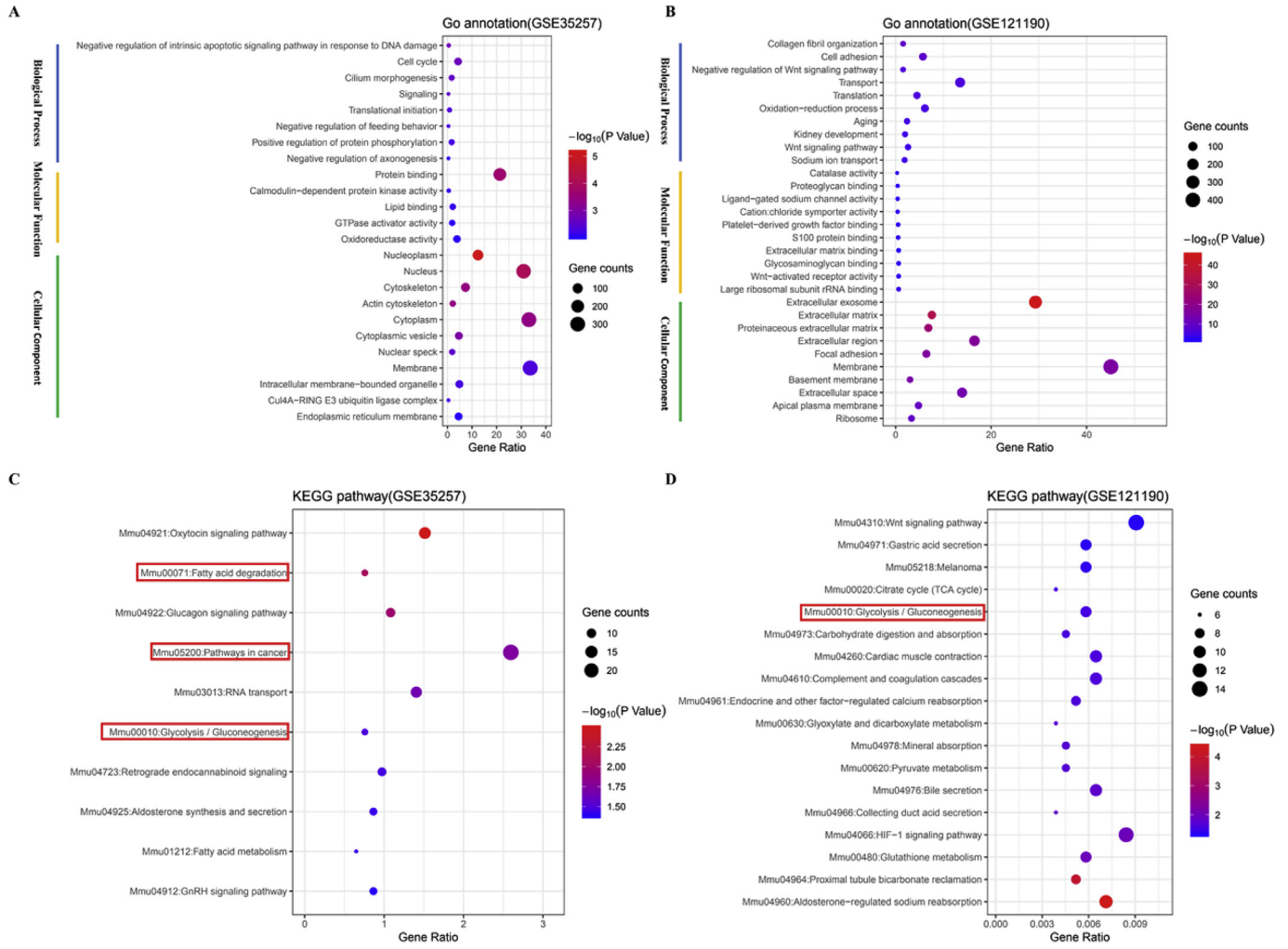

Fig. 3. GO functional and KEGG pathway enrichment analyses of UUO DEGs and cisplatin-induced kidney injury DEGs. A and B) Bubble plot showing the biological processes, molecular functions and cellular components of UUO DEGs and cisplatin-induced kidney injury DEGs, respectively. C and D) Bubble plot showing the KEGG pathways of UUO DEGs and cisplatin-induced kidney injury DEGs, respectively.

import our data and used the Overlay tool to integrate with the previous network, eliminate the genes that are not involved in our dataset. Thus, two network diagram showing changes in gene expression in the UUO and cisplatin-induced model, respectively. The upstream and downstream regulatory network was then showed by using the molecule activity predictor (MAP) overlay tool.

2.7. JASPAR dataset

We obtained the sequence of Aldh2 through the gene database of NCBI (https://www.ncbi.nlm.nih.gov/gene/), and then predicted the binding site with Atf4 on JASPAR database, a high-quality transcription factor binding profile database [14]. Further strengthened our conjecture that Atf4 may be the target gene of Aldh2.

2.8. Animal experiments

Male BALB/C mice (20–25 g, 10 weeks old) were purchased from the Experimental Animal Center of Guangzhou University of Chinese Medicine, housed at 23 ± 2 °C, a 12 h/12 h light/dark cycle and given free access to food and water. All animals adapted to the environment for 1 week before carrying out any experiments.

For the UUO model, mice were anesthetized with 4% chloral hydrate (0. 20 mL/20 g). Through the abdominal incision, the left ureter was tied with fine suture materials (5–0 silk), then cut between the two ligated points to induce a complete obstruction. Kidney tissue were taken 14 days after surgery. Sham-operated mice underwent the same procedure except that the renal ureter was not ligated [6]. For the cisplatin-induced mice model, mice were injected intraperitoneally with a single dose of cisplatin (15 mg/kg) or vehicle (saline) and kidney tissue was taken 3 days after treatment [15]. For the IRI model, mice were anesthetized as mentioned above and renal IRI was performed as previously described. Left renal IRI was clamped to the renal pedicles for 60 min by flank incisions. The clamps were then taken out and the wound sutured after restoration of blood flow was visually observed. Sham-operated mice underwent the same procedure except that the renal pedicles were not clamped [16]. All the above experiments contained 5 males per group.

2.9. Real-time PCR

Kidney tissue was harvested after experiments or sham surgery and immediately frozen on dry ice and stored at −80 °C (n = 5 at each group). Total RNA extracted from rapidly frozen kidney tissue was isolated using Trizol reagent (Invitrogen). Real-time PCR was performed by using TaKaRa SYBR® Premix Ex Taq™ II (Perfect Real Time) to show the expression change of Aldh2 between the experiment group and the control group. Specific primers for Aldh2 was listed in Fig. 5A. Reactions were carried out in a total volume of 20 µl, including 10 µl SYBR® Premix Ex TaqTM(2 ×), 2 µl cDNA, 6.4 dH_2O and 0.8 µl of each

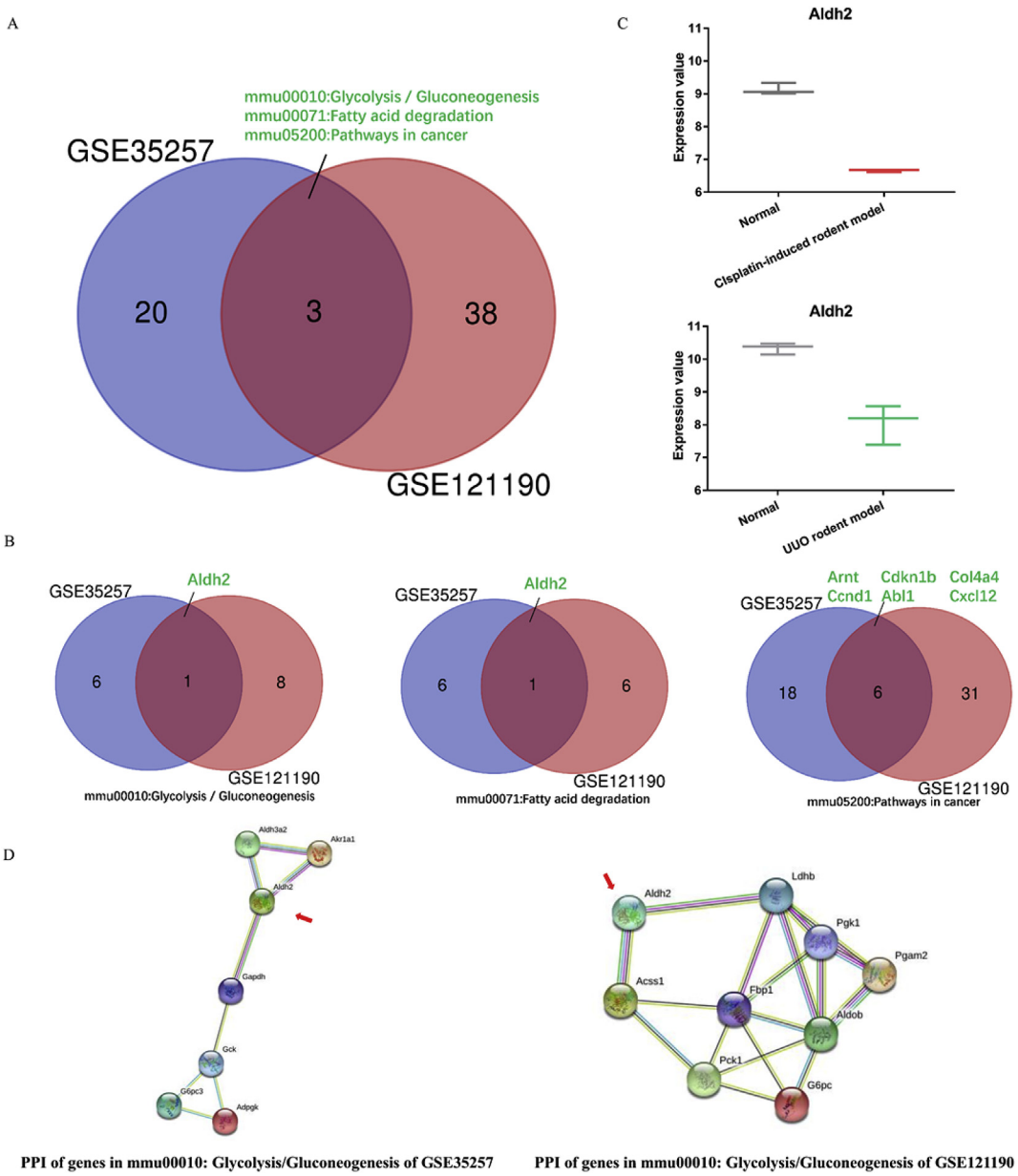

Fig. 4. Aldh2 mediating Glycolysis/Gluconeogenesis pathway in the development of renal fibrosis. A) Venn diagram showing the three shared KEGG pathways of the UUO DEGs and cisplatin-induced kidney injury DEGs. B) Venn diagram showing Aldh2 is the co-genes in glycolysis/gluconeogenesis and fatty acid degradation; while pathways in cancer have 6 co-genes. C) Box plot showing expression change of Aldh2 in the UUO and cisplatin-induced kidney injury, respectively. D) PPI network showing potential interaction of genes involved in glycolysis/gluconeogenesis from two datasets, respectively.

specific primer (10 μM) and run in the ABI PRISM® 7500 Sequence Detection System. The cycling conditions were set at 94 °C for 3–4 min; cycles (30x) at 94 °C for 30 s,60 °C for 30 s and 72 °C for 30 s; the last Cycle(1x) were set 72 °C for 10 min, 16 °C for ∞. β-actin was utilized for standardization. Data were calculated relative to β-actin using the 2-ΔΔCt method.

2.10. Western blotting

Mice kidney tissue was homogenized in a lysis buffer supplemented with 1% protease inhibitor cocktail. Total protein was extracted with RIPA buffer and was used for Western blot analysis. The 20 μg of extracted total protein was separated in SDS-PAGE gel and transferred to PVDF membranes. Following incubation in blocking buffer for 1 h at room temperature, the membrane was incubated at 4 °C overnight with Aldh2 antibody (ab108306, abcam, Cambridge, England). HRP-labeled secondary antibody was used according to the host species of the primary antibody. Western blots were developed using ECL substrate and exposed to x-ray film. β-actin was used for normalization. Then grayscale analysis of Western blotting strips was applied by using Image J.

2.11. Statistical analyses

Statistical analyses were applied using GraphPad Prism 7 and SPSS 23.0. To compare the data between pairs of groups, we then used Paired.Samples Test. All values are shown as mean ± standard deviation (SD). $P < 0.05$ was considered statistically significant.

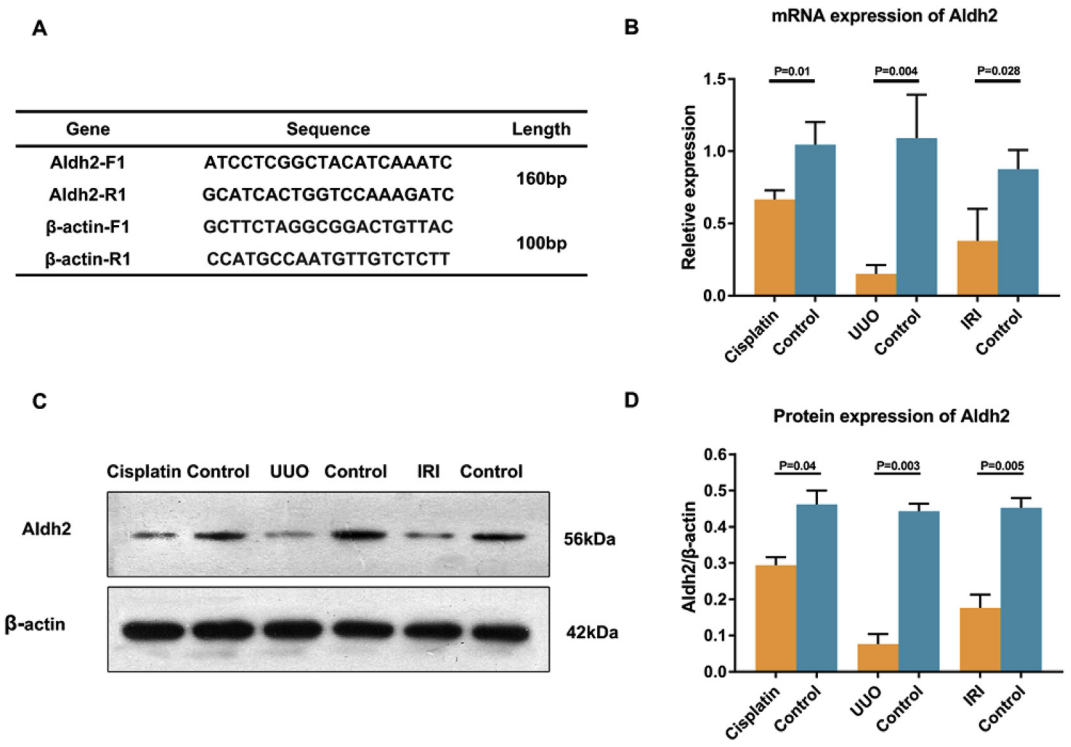

Fig. 5. Gene expression of Aldh2 was validated by rtPCR and western blotting. Fig. 5A Primer sequences for Aldh2; Fig. 5B mRNA expression of Aldh2 were analyzed by rtPCR analysis in three renal fibrosis model. Fig. 5C Protein expression of Aldh2 was analyzed by western blotting (grayscale analysis is shown in D). β-actin as loading control. $P < 0.05$ was considered statistically significant.

Table 1
Enrichment results of three KEGG pathways by GSEA software.

	GS follow link to MSigDB	SIZE	ES	NES	NOM p-val	FDR q-val	FWER p-val	Rank at max	Leading edge	Rank
GSE35257	Glycolysis/gluconeogenesis	31	0.42	**1.1**	**0.3**	**0.722**	1	2106	tags = 26%, list = 13%, signal = 30%	**27**
	Fatty acid metabolism	30	0.34	0.91	0.596	0.821	1	1869	tags = 27%, list = 12%, signal = 30%	46
	Pathways in cancer	140	0.26	0.88	0.761	0.82	1	2304	tags = 19%, list = 14%, signal = 21%	50
GSE121190	Glycolysis/gluconeogenesis	53	0.65	**1.23**	**0**	**0.366**	1	2701	tags = 38%, list = 12%, signal = 43%	**28**
	Fatty acid metabolism	32	0.73	1.3	0	0.44	0.95	2456	tags = 59%, list = 11%, signal = 67%	10
	Pathways in cancer	—	—	—	—	—	—	—	—	—

3. Results

3.1. Data quality assessment and identification of DEGs

Heatmap and unsupervised clustering analysis was used in the GSE121190 and GSE35257 to reveal the distribution of gene expression data of each group (Fig. 1A and Fig. 1B). By using GEO2R online tool, 965 DEGs and 930 DEGs (adj.P < 0.01, $|\log FC| > 1$) were detected from GSE121190 and GSE35257. Volcano plot was used to visualize the UUO DEGs and cisplatin-induced kidney injury DEGs, respectively (Fig. 2B and Fig. 2C). Then UUO (relative to the normal group) DEGs and cisplatin-induced kidney injury (relative to the normal group) DEGs were subjected to Venn analysis to obtain Venn analysis results. Venn diagram showed that 43 co-DEGs were shared (Fig. 2A) and the heatmap was constructed to show the expression change of 43 co-DEGs visually (Fig. 2D). PPI network of 45 co-DEGs was constructed to show the potential gene interaction by STRING database. It revealed that two groups of genes may be hub genes, one group gene is Col4a4, Col18a1 and Col5a3, the other group is Ccnd1, Abl1 and Ckdn1b (Fig. 2E).

3.2. GO functional and KEGG pathway enrichment analyses

GO and KEGG enrichment analysis was performed with two array data separately to identify the most relevant biological processes (BPs), molecular functions (MFs) and cellular components (CC). The significantly represented GO terms with p-value ≤ 0.01 were presented, 85 biological processes were enriched of 965 DEGs while 8 biological processes were enriched of 930 DEGs. The 930 DEGs were mostly enriched related to negative regulation of intrinsic apoptotic signaling pathway in response to DNA damage in BP, protein binding in MF and nucleoplasm in CC term, respectively (Fig. 3A). The 965 DEGs were mostly enriched related to collagen fibril organization in BP, catalase activity in MF and extracellular exosome in CC term, respectively (Fig. 3B). To further research the functions of the DEGs, we represented significant enrichment of the DEGs to the KEGG database. Additionally, the significantly represented KEGG terms with p-value ≤ 0.01 were also presented, the 930 DEGs were considerably enriched in 18 signaling pathways (Fig. 3C) while 965 DEGs were significantly enriched in 10 signaling pathways (Fig. 3D).

3.3. Glycolysis/gluconeogenesis may be a key pathway in the development of renal fibrosis

Comparative analysis of KEGG pathways by bioinformatic approach, a total of 61 KEGG pathways were identified by combining two datasets, 3 KEGG pathways were shared between them, that is glycolysis/gluconeogenesis; fatty acid degradation; pathways in cancer (Fig. 4A). We use GSEA approach to reconfirm the KEGG results, and

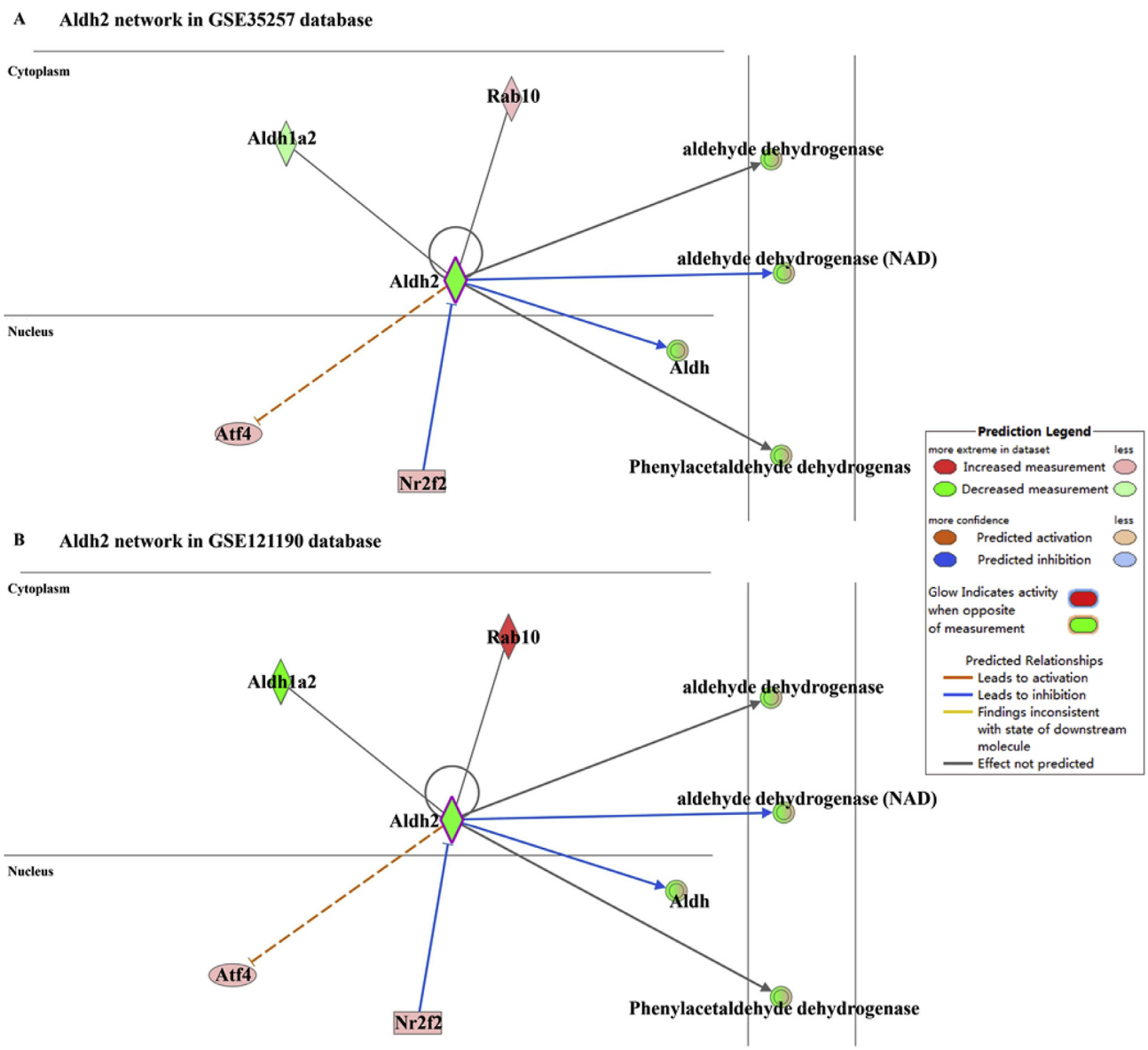

Fig. 6. Interactive regulatory network of Aldh2 in GSE35257 and GSE121190. A and B) The similar interactive regulatory network of Aldh2 in GSE35257 and GSE121190 showing the mechanism promotes renal fibrosis which caused by UUO and cisplatin drug toxics may be identical.

Table 2
Predicting binding site of Aldh2 to the transcription factor Atf4 by JASPAR database.

Name	Score	Relative score	Sequence ID (Aldh2)	Start	End	Strand	Predicted sequence
Atf4	10.7976	0.871696822	NC_000071.6:c121593824-121566027	1799	1811	+	TGCTGAAGCAATC
Atf4	9.84276	0.858339029	NC_000071.6:c121593824-121566027	2314	2326	–	CAATGATGCCACA
Atf4	9.48729	0.8533661	NC_000071.6:c121593824-121566027	1036	1048	–	GGCTGACGGAAGA
Atf4	6.74542	0.815007528	NC_000071.6:c121593824-121566027	1366	1378	+	GTTTGATGCTATA
Atf4	6.63867	0.813514056	NC_000071.6:c121593824-121566027	1741	1753	–	GTATTATGCAAAA

the results from GSEA are basically consistent with the results from DAVID. Furthermore, whether in the GSEA ranking or the NES value, the glycolysis/gluconeogenesis pathway is relatively consistent in two different renal fibrosis models, while the other two pathways are less consistent (Table 1).

3.4. Aldh2 acts as a crucial biomarker in glycolysis/gluconeogenesis pathway in renal fibrosis

Subsequently, we analyzed the related genes in each KEGG pathways by Venn analysis, respectively. We found Aldh2 is the co-genes in glycolysis/gluconeogenesis and fatty acid degradation; while pathways in cancer have 6 co-genes (Fig. 4B). Therefore, we need to confirm whether Aldh2 has a change in expression in UUO and cisplatin-induced kidney injury animal model, suggesting that Aldh2 may be used as a genetic target for renal fibrosis. Box plot show that Aldh2 does have expression change in two kidney injury diseases (Fig. 4C). Next, to understand the potential regulatory network relationship of Aldh2 in the glycolysis/gluconeogenesis pathway, we construct the genes involved in this pathway with STRING and constructed the PPI

network, respectively (Fig. 4D). In order to validate our conjecture that Aldh2 is a common gene target for renal fibrosis with different causes, another IRI renal fibrosis model was chosen. Real-time PCR validation and Western blotting of Aldh2 were applied by comparing normal kidney tissue with three differently treated kidney tissues, respectively. In line with our bioinformatic results, the expression of Aldh2 was most significantly reduced in the UUO model, and then in the IRI model, while the cisplatin-induced model showed a slight decrease in Aldh2 expression (Fig. 5B, C and D).

3.5. Atf4 may be a target gene for Aldh2 by mediating the glycolysis pathway in renal fibrosis

In order to further implicate the relationships of Aldh2 involvement in the interactive protein networks, we used the MAP, a function of IPA that precalculate the upstream/downstream effects of activation or inhibition of molecules included in the analyzed dataset. Using this tool, we established the interactive regulatory network of Aldh2 (Fig. 6A and Fig. 6B). We were able to find that the genes interacted with Aldh2 in UUO and cisplatin-induced kidney injury were similar and their expression change were relatively consistent, suggesting that the mechanism promotes renal fibrosis which caused by UUO and cisplatin drug toxics may be identical. Additionally, the hub genes appeared in the two networks, such as Rab10, Aldh1a2, Atf4, may play important roles in renal fibrosis. However, to our knowledge, none of these kinases have previously been implicated in the pathophysiology of renal fibrosis, but are potential targets for future investigation. Fortunately, we found that Atf4 can be induced by glucose deprivation [17], which may be a target gene of Aldh2 that play important roles in renal fibrosis. In order to strengthen our conjecture, we used the JASPAR database to predict the binding site of Aldh2 to Atf4, and the results showed that they have 5 binding sites (Table 2). Thus, we can speculate that Atf4 acts as a target gene for Aldh2 to mediate the glycolysis pathway, thereby affecting the progression of renal fibrosis.

4. Discussion

Although the causes of chronic kidney disease (CKD) are varied and complex, renal fibrosis is the common final pathological phenotype of all CKD [1]. Exploring the similarities and differences of molecular mechanisms in various renal fibrosis disease will help us to seek breakthrough of treatment with CKD. Obstructive nephropathy and drug toxicity-induced renal injury have different molecular mechanisms despite the same pathologic outcome. However, whether these two renal fibrosis pathogenesis caused by different etiologies have substantial overlap of molecular mechanism between each other, the current research has not been cleared. UUO and the cisplatin induced kidney injury are respectively classical animal models of above two renal fibrosis pathogenesis [3–5]. Therefore, we analysis the existence of shared signaling pathway in these two animal models to explore common key targets in renal fibrosis with different etiologies.

Through the above analysis, we know that glycolysis/gluconeogenesis may be the key biological function whether it's obstructive nephropathy or drug toxicity, indicating that glycolysis/gluconeogenesis may plays a core role in development of renal fibrosis. As we know, glycolysis is the way toward changing over glucose into pyruvate and producing little measures of ATP and NADH, while gluconeogenesis is an amalgamation pathway of glucose from noncarbohydrate precursors. It is basically an inversion of glycolysis with minor varieties of elective ways. Interestingly, research on the study of energy metabolism in renal fibrosis has exploded in the past three years, suggesting that researchers are gradually realizing that energy metabolism plays a significant role in the progression of renal fibrosis. Researches showed that blockade of glycolysis can reduce renal fibrosis in the UUO rodent model [18–21]. Our bioinformatic result suggested that the biological function of glycolysis also plays an important role in the cisplatin-induced renal fibrosis. Therefore, the exact effect of glycolysis in cisplatin-induced renal fibrosis should be verified in the further study. Additionally, the specific mechanism of glycolysis biological function in renal fibrosis is still unclear and requires more in-depth research. As shown above, Aldh2 is the core gene in glycolysis/gluconeogenesis, which indicated that Aldh2 has great effect in the process of renal fibrosis. Notably, researchers have found that Aldh2 plays an important role in the fibrotic effect of different organs, especially in cardiac fibrosis and renal fibrosis. For example, Aldh2 activation was found to play a role in reducing cardiac fibrosis [22], and decrease the HG-induced apoptosis and fibrosis through inhibition of oxidative stress [23]. Additionally, Hammad et al. has demonstrated that Alda1, an Aldh2 agonist can alleviate the expression of biomarkers of renal fibrosis [24]. Hu et al. demonstrated that inhibition of Aldh2 expression aggravates renal injury [25]. These findings are consistent with our bioinformatic analysis, and are also basically consistent with our experimental results. In order to validate our conjecture, Aldh2 is a common gene target for renal fibrosis with different causes. IRI mice model were chosen to join our experiment. Our experiments showed that the expression of Aldh2 was most significantly reduced in the UUO model, and then in the IRI model, while the cisplatin-induced model showed a slight decrease in Aldh2 expression. Overall, the expression of Aldh2 showed a downward trend in renal fibrosis caused by three causes, and the degree of inconsistency was related to many interference factors, such as drug dosage, surgical procedure, and time node selection, etc. Thus, Aldh2 can be considered as novel promising candidates for delving into the mechanism of renal fibrosis. We next used IPA to analyze the star molecule Aldh2 involved in the glycolysis pathway that affects the development of renal fibrosis. Combined with the results of our bioinformatics analysis, we are confident that Aldh2 mediating glycolysis pathway play a crucial role in the progression of renal fibrosis.

Notably, among the interaction molecules of Aldh2 we showed, it found that Activating transcription factor 4 (Atf4) can be induced by glucose deprivation [17], which was predicted to be a target gene of Aldh2 that have effects in the renal fibrosis by mediating the glycolysis pathway. Atf4 is a famous gene that encodes a transcription factor and was initially distinguished as a broadly expressed mammalian DNA binding protein, involving diverse cellular activities. Previous research has investigated that upregulation of Atf4 protein expressions in UUO rat can affect the development of renal fibrosis [26], followed by reducing glucose regulated protein 78 (GRP78) [27]. The results also indicated that Atf4 take part in the glycolysis pathways. However, the role of Atf4 in glycolysis pathway remains largely unclear and needs further research. Additionally, all relevant studies have focused on obstructive nephropathy and little attention has been paid to drug toxicity induced renal fibrosis. Therefore, there is still a long way to further study in renal fibrosis with different etiologies.

5. Conclusion

In summary, our comprehensive analysis in the assays of two different model identified glycolysis/gluconeogenesis as a common key biological function in the development of renal fibrosis. What's more, Aldh2 was demonstrated to act as a potential genetic target for renal fibrosis. Further experiments could be performed to validate the specific mechanism of Aldh2, as the results showed by bioinformatics analysis, Aldh2 may play roles by mediating glycolysis pathway via targeting Atf4. Our bioinformatics analysis of renal fibrosis models with different etiologies will be a valuable resource for illuminating the molecular mechanism underlying renal fibrosis processing.

Data availability statement

The data that support the findings of this study are downloaded from the Gene Expression Omnibus (GEO) database (https://www.ncbi.nlm.nih.gov/geo/query/acc.cgi; GEO accession:GSE35257;

GSE121190).

Author contributions

Simin Tang and Teng Huang contributed equally to this work. Simin Tang carried out the conception and the derivation of the study, carried out the bioinformatics analysis and drafted the manuscript with the help of Jun Zhou. Teng Huang performed the animal experiments, real-time PCR, western blotting and modify the manuscript. Huan Jing generate the data from the GEO and analyze the data preliminarily. Zhenxing Huang performed the animal experiments and helped to modify the manuscript. Hongtao Chen, Youling Fan and Jiying Zhong guided the general research strategy and gave the critical revision of this manuscript. All authors read and approved this manuscript.

Declaration of competing interest

The authors declare that there are no conflicts of interest.

Acknowledgement

This work was supported by the grant from National Natural Science Foundation of China (8186013); Foshan Science and Technology Bureau (2017AB001441) and Foshan Department of Health (20160075).

References

[1] P. Boor, T. Ostendorf, J. Floege, Renal fibrosis: novel insights into mechanisms and therapeutic targets, Nat. Rev. Nephrol. 6 (11) (2010) 643–656.
[2] A. Nogueira, M.J. Pires, P.A. Oliveira, Pathophysiological mechanisms of renal fibrosis: a review of animal models and therapeutic strategies, Vivo 31 (1) (2017) 1–22.
[3] M. Perse, Z. Veceric-Haler, Cisplatin-induced rodent model of kidney injury: characteristics and challenges, BioMed Res. Int. 2018 (2018) 1462802.
[4] R.L. Chevalier, M.S. Forbes, B.A. Thornhill, Ureteral obstruction as a model of renal interstitial fibrosis and obstructive nephropathy, Kidney Int. 75 (11) (2009) 1145–1152.
[5] N. Pabla, Z. Dong, Cisplatin nephrotoxicity: mechanisms and renoprotective strategies, Kidney Int. 73 (9) (2008) 994–1007.
[6] A.Y. Higashi, B.J. Aronow, G.R. Dressler, Expression profiling of fibroblasts in chronic and acute disease models reveals novel pathways in kidney fibrosis, J. Am. Soc. Nephrol. 30 (1) (2019) 80–94.
[7] L.T. Zhou, et al., Integrative bioinformatics analysis provides insight into the molecular mechanisms of chronic kidney disease, Kidney Blood Press. Res. 43 (2) (2018) 568–581.
[8] L.T. Zhou, et al., Feature selection and classification of urinary mRNA microarray data by iterative random forest to diagnose renal fibrosis: a two-stage study, Sci. Rep. 7 (2017) 39832.
[9] S. Davis, P.S. Meltzer, GEOquery: a bridge between the gene expression Omnibus (GEO) and BioConductor, Bioinformatics 23 (14) (2007) 1846–1847.
[10] W. Huang da, B.T. Sherman, R.A. Lempicki, Systematic and integrative analysis of large gene lists using DAVID bioinformatics resources, Nat. Protoc. 4 (1) (2009) 44–57.
[11] A. Subramaniana, et al., Gene set enrichment analysis: a knowledge-based approach for interpreting genome-wide expression profiles, Proc. Natl. Acad. Sci. 102 (2005) 15545–15550.
[12] V.K. Mootha, et al., PGC-1α-responsive genes involved in oxidative phosphorylation are coordinately downregulated in human diabetes, Nat. Genet. 34 (3) (2003) 267–273.
[13] D. Szklarczyk, et al., STRING v11: protein-protein association networks with increased coverage, supporting functional discovery in genome-wide experimental datasets, Nucleic Acids Res. 47 (D1) (2019) D607–D613.
[14] A. Khan, et al., Jaspar 2018: update of the open-access database of transcription factor binding profiles and its web framework, Nucleic Acids Res. 46 (D1) (2018) D260–D266.
[15] C.G. Lee, et al., Discovery of an integrative network of microRNAs and transcriptomics changes for acute kidney injury, Kidney Int. 86 (5) (2014) 943–953.
[16] M. Liu, et al., Effects of delayed rapamycin treatment on renal fibrosis and inflammation in experimental ischemia reperfusion injury, Transplant. Proc. 41 (10) (2009) 4065–4071.
[17] C.L. Leon-Annicchiarico, et al., ATF4 mediates necrosis induced by glucose deprivation and apoptosis induced by 2-deoxyglucose in the same cells, FEBS J. 282 (18) (2015) 3647–3658.
[18] Q W, et al., Glycolysis inhibitors suppress renal interstitial fibrosis via divergent effects on fibroblasts and tubular cells, Am. J. Physiol. Renal. Physiol. 316 (4) (2019) F615–F767.
[19] M L, et al., Elevated aerobic glycolysis in renal tubular epithelial cells influences the proliferation and differentiation of podocytes and promotes renal interstitial fibrosis, Eur. Rev. Med. Pharmacol. Sci. 22 (2018) 5082–5090.
[20] H. Ding, et al., Inhibiting aerobic glycolysis suppresses renal interstitial fibroblast activation and renal fibrosis, Am. J. Physiol. Renal. Physiol. 313 (3) (2017) F561–F575.
[21] X.-N. YIN, et al., Enhanced glycolysis in the process of renal fibrosis aggravated the development of chronic kidney disease, Eur. Rev. Med. Pharmacol. Sci. 22 (2018) 4243–4251.
[22] Q. Yuan, et al., ALDH2 activation inhibited cardiac fibroblast-to-myofibroblast transformation via the TGF-beta1/smad signaling pathway, J. Cardiovasc. Pharmacol. 73 (4) (2019) 248–256.
[23] X. Gu, et al., Effect of ALDH2 on high glucose-induced cardiac fibroblast oxidative stress, apoptosis, and fibrosis, 2017 Oxid Med Cell Longev, 2017, p. 9257967.
[24] F.T. Hammad, et al., Alda-1, an aldehyde dehydrogenase-2 agonist, causes deterioration in renal functions following ischemia-reperfusion injury due to crystalline nephropathy, Drug Dev. Res. 79 (7) (2018) 315–323.
[25] J.F. Hu, et al., Inhibition of ALDH2 expression aggravates renal injury in a rat sepsis syndrome model, Exp. Ther. Med. 14 (3) (2017) 2249–2254.
[26] C. Zhang, et al., Regulation of eIF2alpha expression and renal interstitial fibrosis by resveratrol in rat renal tissue after unilateral ureteral obstruction, Ren. Fail. 38 (4) (2016) 622–628.
[27] S.-H. Liu, et al., Chemical chaperon 4-phenylbutyrate protects against the endoplasmic reticulum stress-mediated renal fibrosis in vivo and in vitro, Oncotarget 7 (2016) 22116–22127.